

# Effects of Density Currents on Sedimentation in Reservoirs

B.A. Mohammadnezhad<sup>1</sup> and A. Shamsai\*

The development of density or turbidity currents causes serious problems for environmental hydraulics in reservoirs. The stream entered to a reservoir can carry sediments, nutrients and chemicals as density or turbidity currents. The fate of sediment and other substances transported by the current depends on the characteristics of the turbidity current itself, i.e. the velocity of fluid, the amount of mixing with reservoir water and the rates of sediment deposition and re-suspension. These are important factors for water quality in reservoirs. A two-dimensional, depth-averaged, finite-volume numerical model is developed to study density currents, driven by non-cohesive sediments. The model has been, then, run with variant input conditions, which could be assessed for their effects on the development of bed and sediment deposits. The amount of sediment deposition and the grain size of deposits have been found to decrease uniformly with their distance from the inlet. The numerical results are compared with some experimental data of turbidity currents and a favorable general agreement is observed

## INTRODUCTION

A wide variety of geophysical and engineering flows are classified as density currents. Examples include katabatic winds, dust storms, saltwater intrusions in estuaries, convective currents in lakes and reservoirs, hyperpycnal plumes due to 'dirty' rivers flowing into oceans and dense vapor clouds emitted by industrial stacks [1-5]. A turbidity current is a particular type of density current, which occurs in oceans and lakes bottoms [6]. The driving force of a turbidity current is due to the particulate phase, i.e. suspended sediment, which renders the flowing turbid water heavier than clear water [7]. A submarine density current can also occur by the thermal stratification and salinity gradient. Along flows, turbidity currents exchange sediments with erodible beds through erosion and deposition. Turbidity currents often represent a hazard, i.e. create inappropriate conditions, which can place man's underwater activities at considerable risk [8].

Initial observations on lacustrine turbidity currents were made by Forel [9] in Geneva Lake. Some recent significant observations have been made on turbidity currents in Switzerland, in Geneva and Constance

Lakes [10,11]. There have also been numerous research efforts to understand the mechanics of density currents, in general. Most experimental work undertaken on density currents flowing along inclined or horizontal boundaries have concentrated on conservative cases, for which the factor of the density difference is neither lost nor gained along the flow. Some examples are: Ellison and Turner [12], Simpson and Britter [13] and Britter and Linden [14]. Turbidity currents are, however, intrinsically non-conservative in the sense that sediment can be gained by erosion or lost by deposition. Several investigations have been undertaken which have treated turbidity currents as purely depositional cases [15-18], that is currents for which erosion and deposition occur simultaneously [17,19,20] and currents that are locally neither depositional nor erosional [21,22]. All these experiments are two-dimensional, allowing variability in the stream-wise and normal directions. Fietz and Wood [23] and Tsihrintzis and Alavian [3] studied three-dimensional spreading of conservative currents, experimentally.

There are also several models for turbidity currents, which allow simultaneous deposition and erosion of sediment [8,18,24-35]. These models have not revealed the causative mechanism for self-canalization of submarine fans, since they had not allowed any variation in the lateral direction. In order to describe the inception of a channel from a depositional turbidity current, a variation of flow and deposit in a lateral

---

1. *Department of Civil Engineering, Sharif University of Technology, Tehran, I.R. Iran.*

\*. *Corresponding Author, Department of Civil Engineering, Sharif University of Technology, Tehran, I.R. Iran.*

direction should be allowed. Simpson [36,37] and Garcia [7] give a good overview of turbidity currents.

The method applied in this work employs 2D, vertically averaged, time-dependent equations, including fluid, sediment and the momentum conservation law, as the basis for a turbidity current model. These equations are significantly less complicated than full hydrodynamic equations, because they are accurate enough to study the development of bathymetry due to turbidity current flows and the transport of suspended sediments. The use of vertically averaged equations implies that vertical accelerations are negligible. This is reasonable to most flows in a submarine environment, because of small bed slopes typically found there. In addition, a bed change equation, is also solved in order to track the bed development. It is essential to know that the bed can have a dramatic impact on the hydrodynamics of turbidity currents and on its complex interaction with its surroundings.

The goal of this paper is to develop a novel numerical model to simulate turbidity currents in a reservoir. Moreover, the effects of inflow conditions are assessed in the development of the bed and sediment deposits via changing the inflow conditions in a reasonable range. Previous attempts at turbidity current modeling in a sub-aqueous environment have been limited, primarily to either one spatial dimension or steady state conditions. In addition, sedimentation has been often neglected, severely limiting the applicability of such models. The improved features of the present model allow the observation and analysis of novel phenomena, which are beyond the capabilities of previous models. Thus, this paper presents an original attempt to evaluate the effects of sediment supply, sediment properties, inflow conditions and basin geometry on the mechanics of turbidity currents and sediment deposits.

## DESCRIPTION OF DENSITY CURRENTS IN RESERVOIRS

A density current is formed when water flowing into a lake or reservoir has a different density from the lake water. The density difference,  $\Delta\rho$ , can be due to the following:

1. Temperature variation:  $\Delta\rho \cong 2 \left[ \frac{kg}{m^3} \right]$ ,
2. Salinity:  $\Delta\rho \cong 20 \left[ \frac{kg}{m^3} \right]$ ,
3. Sediment concentration:  $\Delta\rho \cong 20 \sim 200 \left[ \frac{kg}{m^3} \right]$ .

A combination of the effects has been also observed. In the case of temperature difference, if the density of inflow is less than that of the lake, the current will approach the water surface. If inflow density is higher than that of the lake water, the current will move

along the lake bed. In a stratified lake, it is possible that the current move down into the water body at a temperature equal to the temperature of inflowing water.

A density current caused by high sediment concentration is called a turbidity current. *Videlicet*, turbidity currents are flows driven by density differences caused by suspended fine solid materials. They belong to the family of sediment gravity currents. These are sediment-laden flows that move down slope in still waters, like oceans, lakes and reservoirs. Their driving force is gained from suspended materials, which renders the flowing turbid mixture heavier than the surrounding water and its entering into the lake depends on density differences. Turbidity currents are often encountered when a sediment-laden tributary enters a lake or reservoir (Figure 1). They can transport sediments a long way into the reservoir and can even cause deposits in front of an intake in a large reservoir.

Along the upper reaches of a reservoir, stable, floating debris will be observed, indicating the so-called "plunge point", where the inflowing river stream changes into a density current. The stationary position of the debris is caused by slow (or near zero velocity) upstream movement of the overlying water mass, just downstream of the point where the sediment-laden inflow dives below the water surface. Under unfavorable boundary conditions, the density current could be broken up, either by turbulent mixing in certain parts of the reservoir or by deposition of sediments, whereby the density difference decreases, due to the driving of the density current.

Density currents occur, not only in reservoirs on heavily silt-laden rivers (such as the Eril Emda Reservoir in Algeria, Lake Mead in the USA, the Sanmenxia Reservoir in China and the Sefid Roud and Dez Reservoirs in Iran), but also in reservoirs with flows containing low sediment concentrations (such as the Sautet Reservoir in France).

## GOVERNING EQUATIONS

Turbidity currents occur as underflows in deep seas and reservoirs. When flow thickness does not exceed about 7.5 percent of the overall ambient fluid depth,

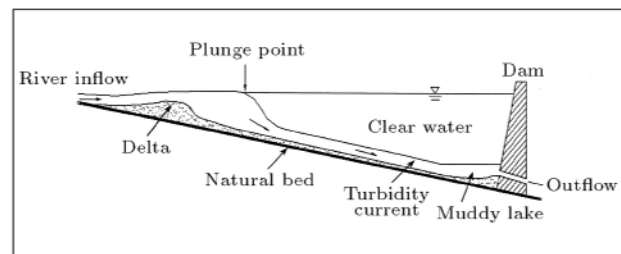


Figure 1. Turbidity current entering a reservoir.

the hydrodynamics of the turbidity current can be accurately described by a “single-layer” formulation [38]. The Equations which form the basis of the model are vertically-averaged, fluid, momentum and sediment conservation equations. These equations form a coupled system of nonlinear, hyperbolic, partial differential equations, which are mathematically similar to shallow water equations. They are valid for flows of a two-dimensional turbidity current driven by uniform, non-cohesive sediments and the flow beneath an infinitely deep layer of quiescent fluid, so, they are written, as follows [6]:

$$\frac{\partial U}{\partial t} + \frac{\partial F}{\partial x} + \frac{\partial G}{\partial y} = Q, \quad (1)$$

where  $U^T = (h, hU, hV, hC)$  is the vector of conservation variables and:

$$F = \begin{bmatrix} hU \\ hU^2 + \frac{1}{2}g'Rh^2C \\ hUV \\ hUC \end{bmatrix}, \quad (2)$$

$$G = \begin{bmatrix} hV \\ hUV \\ hV^2 + \frac{1}{2}g'Rh^2C \\ hVC \end{bmatrix}, \quad (3)$$

$$Q = \begin{bmatrix} E_w \sqrt{U^2 + V^2} \\ ghRCs_x \quad C_D U \sqrt{U^2 + V^2} \\ ghRCs_y \quad C_D V \sqrt{U^2 + V^2} \\ w_s \cos \theta (E_s - c_b) \end{bmatrix}, \quad (4)$$

where  $h$  = flow thickness,  $U$  and  $V$  = depth-averaged velocities in the  $x$  and  $y$  directions, respectively,  $C$  = depth-averaged volume concentration of the sediment,  $E_w$  = fluid entrainment coefficient,  $E_s$  = sediment entrainment coefficient,  $w_s$  = settling velocity,  $c_b$  = near-bed concentration of sediment,  $C_D$  = bed drag coefficient,  $S_x, S_y$  = bed slopes in the  $x$  and  $y$  directions, respectively;  $R = (\rho_s - \rho)/\rho$  with  $\rho_s$  and  $\rho$  being the densities of sediment and ambient water, respectively and  $g' = g \cos \theta$ , with  $\theta$  being the angle between the bed-normal direction and the vertical axis.

The assumptions made in deriving the governing equations include the Boussinesq approximation and small vertical variations. It is also assumed, in the two-dimensional extension, that the coefficients, arising from non-uniformities of velocity and concentration distributions in the vertical direction, are equal to unity. The justification of this assumption is given in Choi [39]. It is interesting to note that the continuity and the momentum equations are analogous to shallow water equations for surface water, except for hydrostatic pressure terms, which are essentially reduced by  $Rc$ , in governing equations, for turbidity currents.

Since only the lower dense layer has been considered in governing equations, the equations represent a single-layer model.

In the present work, the terms describing the diffusion of momentum due to turbulence are considered negligible and are not included in the equations.

The elevation of the bed is a consequence of mud deposition from the current and, thus, the sediment-laden flow. Hence, deposition from the flow changes the bed morphology and the resulting change in the bed slope changes the flow. The elevation of the bed is computed from Exner's equation [40]:

$$(1 - \lambda) \frac{\partial \eta}{\partial t} = w_s (c_b - E_s), \quad (5)$$

where,  $\eta$  denotes the elevation of the bed from a certain datum and  $\lambda$  is the porosity of the deposited sediment particles.

## CLOSURE RELATIONS

In order to solve the governing equations, some basic properties of turbidity currents are needed. Those include, e.g., entrainment of ambient fluid from above, sediment entrainment from the reservoir bed into the current body, flow resistance and sediment deposition. Parker et al. [28] conducted some experiments to observe the behavior of continuous silt-laden turbidity currents over a bed of similar sediment. They established approximated similarity laws for the velocity and sediment concentration distribution, with the help of experimental data, and estimated several shape factors. Based on their experimental data, the following relationship has been proposed to calculate the water entrainment coefficient:

$$E_w = \frac{0.075}{\sqrt{1 + 718R_i^{2.4}}}, \quad (6)$$

where,  $R_i$  is the Richardson number, defined as  $R_i = \frac{ghRC}{U^2 + V^2}$ . An expression for  $E_s$  has been developed as follows [25]:

$$E_s = \frac{1.3 \times 10^{-7} Z^5}{1 + 4.3 \times 10^{-7} Z^5}, \quad (7)$$

where,  $Z = \sqrt{u_*^2 + v_*^2}/w_s f(R_p)$ , with  $f$  being a function of the particle Reynolds number,  $R_p = \frac{d_{50} \sqrt{gRd_{50}}}{\nu}$ , i.e.:

$$f(R_p) = \begin{cases} R_p^{0.6} & R_p \geq 3.5 \\ 0.586R_p^{1.23} & 1 < R_p < 3.5 \end{cases}. \quad (8)$$

The reference concentration ( $c_b$ ) is evaluated close to the bed,  $b \cong 0.05h_t$ , by [38]:

$$\frac{c_b}{C_s} = f\left(\frac{u_{*b}}{w_s}\right), \quad (9)$$

where,  $C_s$  is the concentration defined by the integral scale. From experiments with turbidity currents [41,28], it is found that  $c_b/C_s \cong 2$ . This value remains more or less constant for  $1 < u_{*b}/w_s < 50$ .

The settling velocity,  $w_s$ , can be calculated, as follows:

$$w_s = \frac{d_{50}^2 g R}{18\nu}, \quad (10)$$

where,  $d$  is the particle diameter and  $\nu$  is the viscosity of the fluid.

## NUMERICAL SCHEME AND BOUNDARY CONDITIONS

A second-order accurate Monotone Upstream Scheme for Conservation Laws (MUSCL) [42] is used to solve the governing equations. The Roe's approximate Riemann solver is used for flux vector splitting. This scheme is monotone and does not produce any oscillations. The numerical diffusion of this scheme is very low and, so, it does not significantly reduce the length of the recirculation zone. Typical boundary conditions used in this study are solid wall, outflow and specified inflow. The implementation of boundary conditions is accomplished by the use of a ghost cell at the boundary, but, one outside the domain of interest. By placing the appropriate quantities in the ghost cell, the flux at the boundary can then be solved in the manner.

## NUMERICAL AND EXPERIMENTAL RESULTS

A numerical model is used to simulate experimental cases of 1D and 2D turbidity currents. In the one-dimensional case, the model computations are performed to simulate the experimental observations of turbidity currents developing on an inclined bed. The flume length is 12 m and the initial gate height,  $h_0 \approx 4.0$  (cm), is maintained through all experiments. Altınakar et al. [41] and Garcia [18] experimentally investigated weakly depositing turbidity currents in the flume of a slope angle in the range of  $0 \leq \theta \leq 2.073^\circ$  with two different sizes of sediment. Several numerical test cases have been used for validation and verification of the model. Some cases have been selected, which are presented in Table 1.

An example of computational results with data achieved from Exp. 19, showing the profiles of current height, velocity and concentration in the longitudinal direction, is given in Figure 2. The computational results of Exp. 19 have been compared to the results achieved by Choi and Garcia [40] through this figure. Figure 3 also shows the downstream variations in the amount of sediment deposited per unit bed area by turbidity currents. In made experiments, the

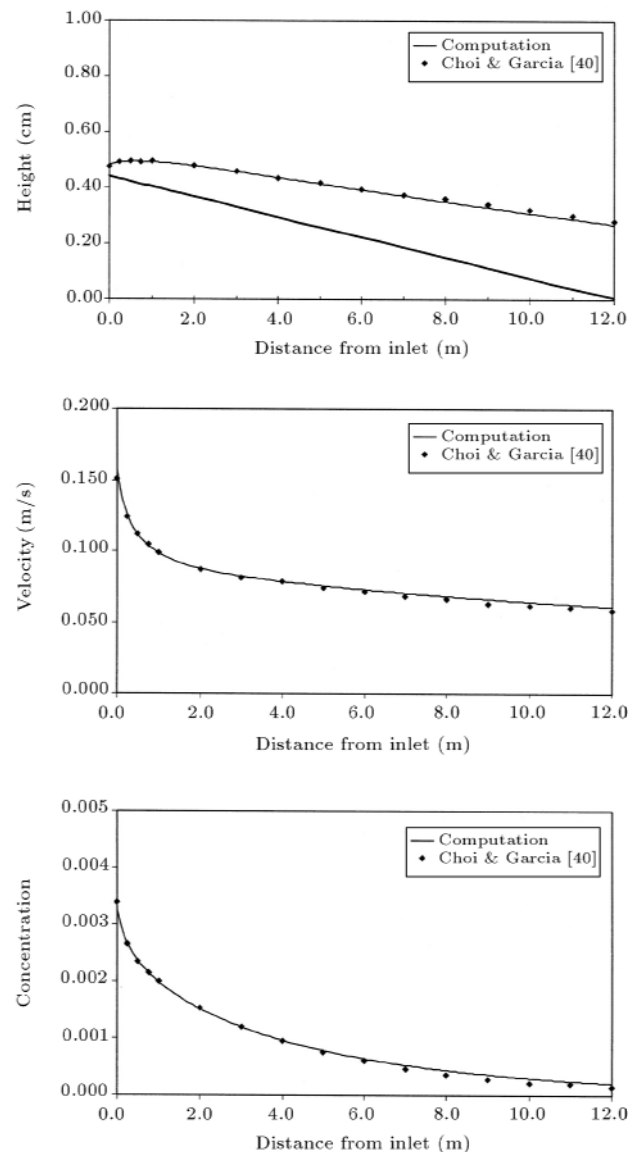


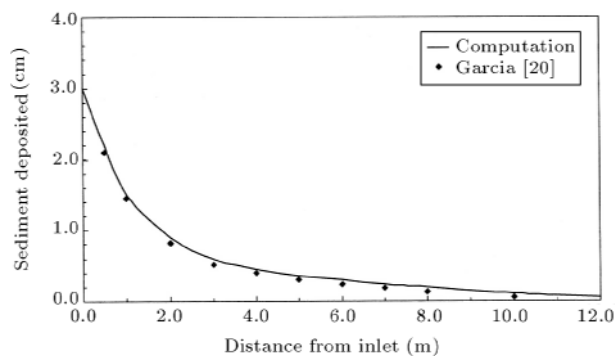
**Figure 2.** Propagation of a turbidity current on a sloping bed (Exp. 19).

corresponding running time for GLASSA2 is recorded as 28 min [43]. This time is sufficient to see well developed steady currents. The value of porosity  $\lambda = 0.5$ , as measured in the laboratory, has been used in computations. Computed profiles well agree with measured data. However, numerical predictions tend to exaggerate the amount of sediment deposition near the inlet where the underflows initiate.

Locations of the current front from the inlet are plotted as a function of time in Figure 4. Numerical predictions have been compared in this figure, with observations man made in two experiments by Altınakar et al. [41]. Initially, the numerical fronts are seen to travel faster than the observed ones. However, after the initial stage, the mean speeds of computed and observed fronts seem to agree well. A better fit of the

**Table 1.** Inlet conditions of experimental and numerical tests.

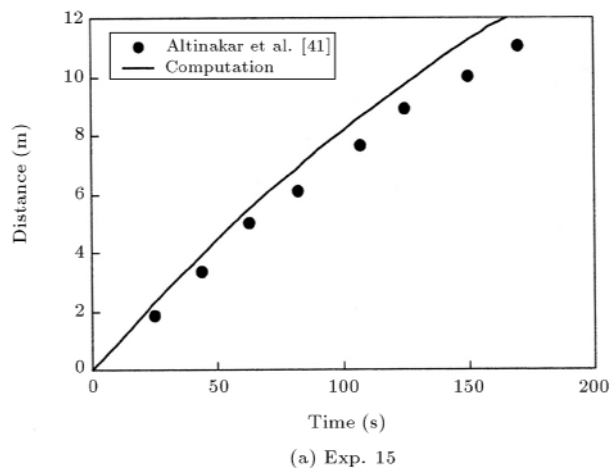
Test Case	Discharge ( $\text{cm}^2/\text{s}$ )	Particle Diameter (mm)	$h_0$ (cm)	Bed Slope Angle	Concentration
Run 1	50	0.03, 0.05, 0.10	4	2	0.006
Run 2	50	0.05	4	1, 2, 3	0.006
Run 3	50	0.05	4	2	0.003, 0.006, 0.009
Run 4	50, 75, 100	0.05	4	2	0.006
Exp. 15 [41]	65	0.032	4	1.203	0.0037
Exp. 19 [41]	64	0.032	4	2.073	0.0034
GLASSA8 [43]	33	0.003	3	2.073	0.0055

**Figure 3.** Pattern of sediment deposited by turbidity currents (GLASSA8).

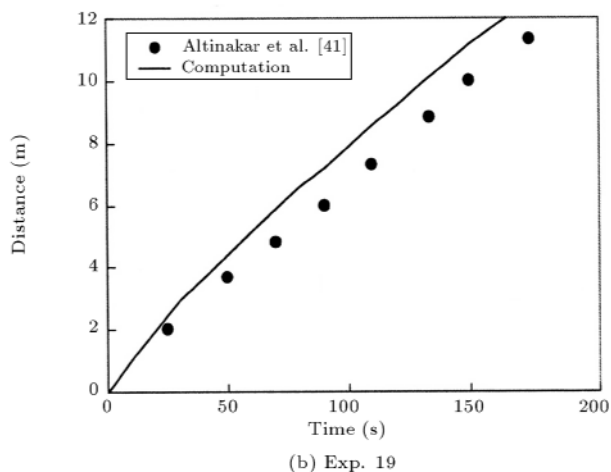
observations could be obtained through adjusting the bed friction coefficient, although it is not the purpose of numerical computations.

In two-dimensional cases, a developed numerical model is applied to laboratory experiments by Luthi [44]. The tank used in the experiment is 6 m wide, 10 m long and 1 m deep. An inlet box with an entry slot (30 cm wide and 5 cm high) is located at the upper end of the tank and, through this entry slot, the turbidity currents are released on a sloping surface, which has been held at a constant inclination of  $5^\circ$  inside the tank. The initial flow variables were  $q_0 = 116 \text{ cm}^2/\text{s}$ ,  $C_0 = 0.05$  and particle size  $D_s = 37 \mu$  ( $\nu_s = 0.082 \text{ cm/s}$ ). A flow resistance coefficient,  $c_D = 0.005$ , and a sediment entrainment coefficient,  $E_s = 0$ , have been kept constant throughout the computations.

Figure 5 shows the propagation of a two-dimensional turbidity current and velocity vectors at different times after being discharged on a sloping bed. The velocity vector fields properly represent radially propagating turbidity current features. This also suggests that the simulated turbidity current is an example of decelerating-depositional underflow. The computed spreading patterns have been well compared to the recorded ones by Luthi [44]. It is interesting to note that the depth-averaged thickness of the current does not increase significantly along the downstream



(a) Exp. 15



(b) Exp. 19

**Figure 4.** Simulated travel distance of turbidity currents.

direction due to lateral spreading, although there is a considerable amount of water entrainment of the ambient layer.

Figure 6 shows contour plots of volumetric concentrations computed from the numerical model at different times. The turbidity current is diluted by entraining of the ambient water through the interfacial area increased by the lateral spreading.

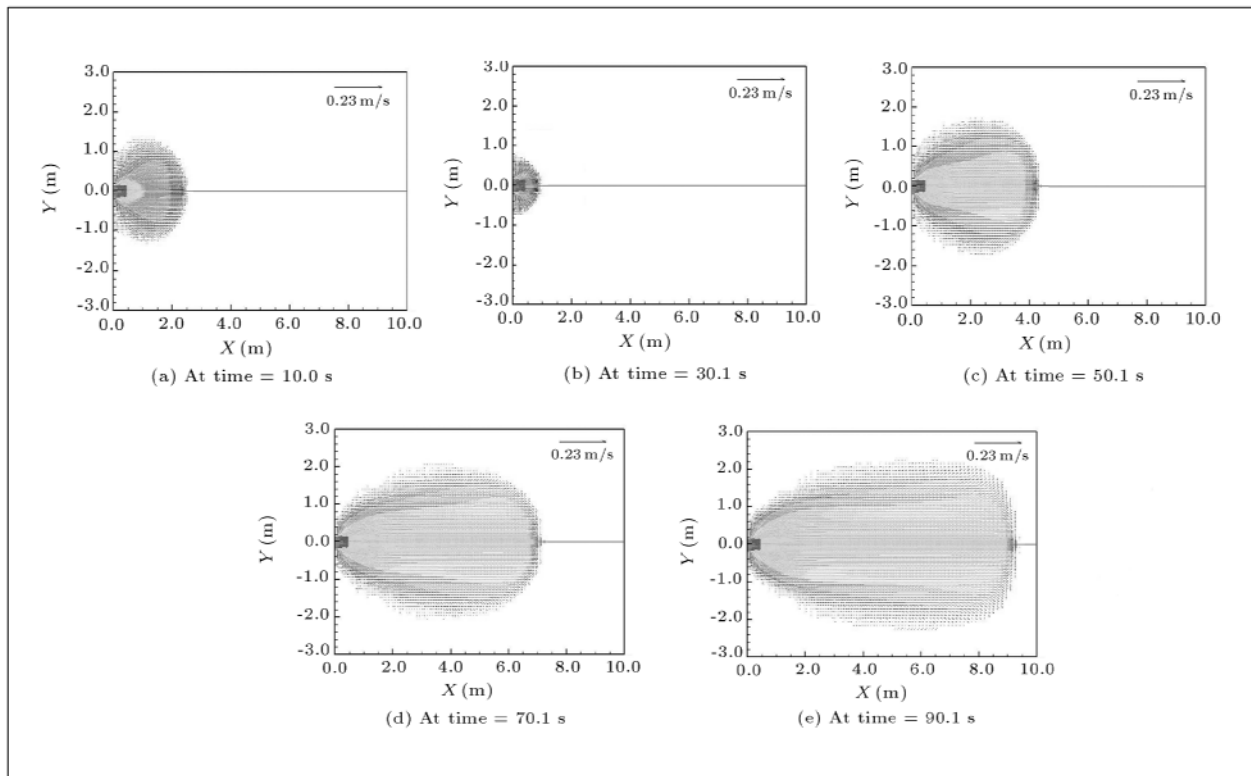


Figure 5. Turbidity current velocity vectors.

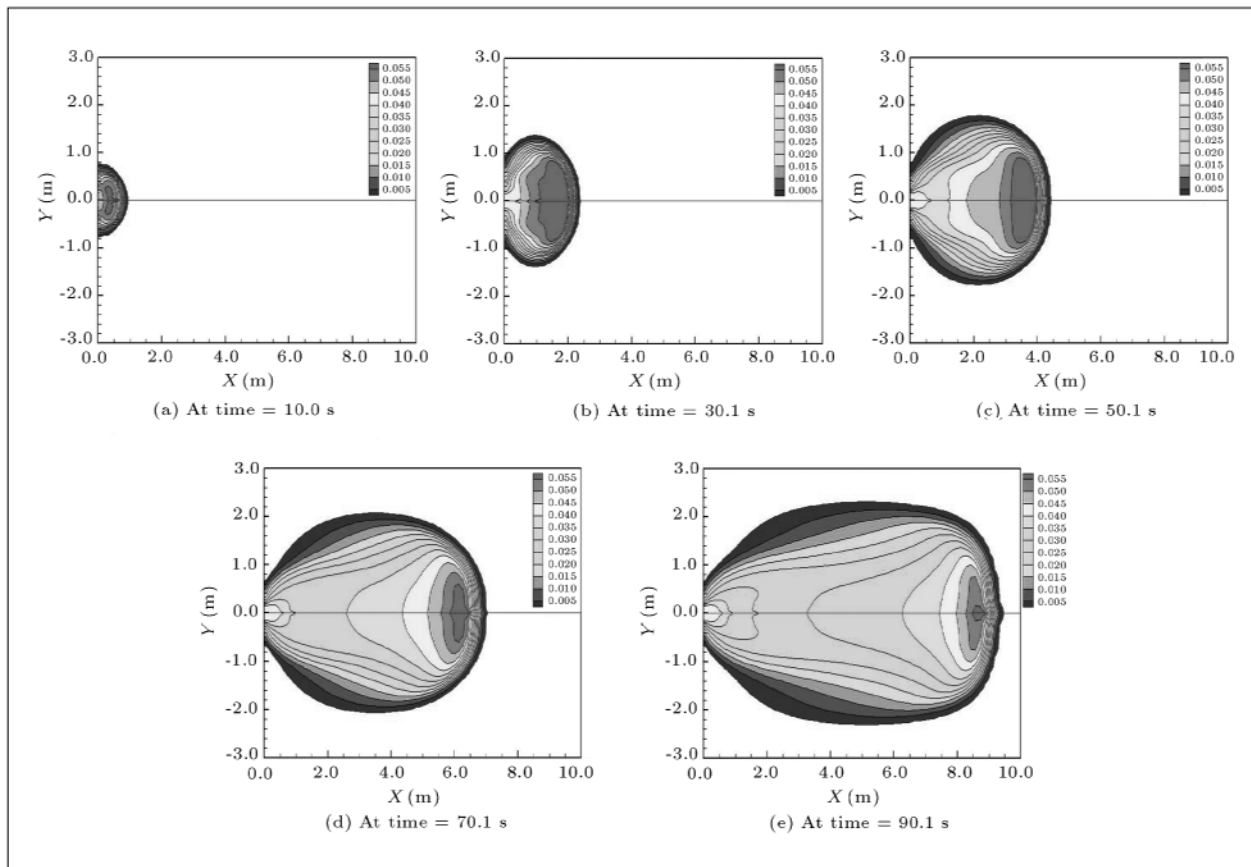


Figure 6. Turbidity current volumetric concentration.

## SENSITIVITY ANALYSIS OF PARAMETERS

The sensitivity of the spreading rates to various parameters in the numerical model is shown in Figure 7, for both longitudinal and lateral directions. This figure shows that higher total buoyancy flux ensures faster spreading in both directions. This is consistent with experimental observations made by Tsihrintzis [3]. The impact of the inlet velocity in Figure 7 is obtained from density currents having the same total buoyancy flux but different volume fluxes at the inlet. It is observed that the inlet velocity hardly affects the longitudinal spreading rate. However, the lateral spreading rates appear to be slightly influenced by the inlet velocity. This can be explained by the fact that the lateral expansion is affected by the volume flux, as well as by the total buoyancy flux.

Figure 7 also shows the impact of the flow resistance coefficient on two dimensional spreading in various slopes. The resistance coefficient,  $C_D$ , appears to retard the propagation in both longitudinal and lateral directions.

The dependence of the slope on the spreading rate has been also seen in Figure 7. The higher the bottom slope,  $S_x$ , in the longitudinal direction, the faster the density current propagates downstream. On the other hand, the situation would be reversed in the lateral direction. That is, the lateral spreading is faster on the less sloped bottom, which is intuitively reasonable, because the lateral spreading hinders the longitudinal spreading.

The impact of sediment particle size within the turbidity current on two dimensional spreading is given in this figure. As particle size grows, causing the particle fall velocity to increase, the deceleration of the current will be noticed in both directions, due to the loss of buoyancy.

As a result, the longitudinal spreading rate of

the density current is found to be more sensitive to the total buoyancy flux rather than to the slope,  $S_x$ . Two-dimensional propagations are observed to be insensitive to the flow resistance coefficient and the particle settling velocity and these two parameters seem to be quite sensitive.

## EXPERIMENTAL VERIFICATION OF 2D NUMERICAL MODEL

A series of experiments are conducted on a three-dimensional flume in the Hydro-systems Laboratory at the University of Illinois. The purpose of these experiments is to obtain data on the two-dimensional spreading of density currents. A wooden flume (8 ft wide, 12 ft long and 4 ft deep) has been used for the experiments. The fractional depth (flow depth to total depth ratio) at the inlet is set to 0.1, which is intended to prevent any dynamic effect from the overlying fluid layer.

Table 1 summarizes experimental conditions and initial flow parameters at the inlet. The inlet is 3 cm high and 10 cm wide.

Figure 8 shows propagating patterns in plan view from DEN3 and DEN6, respectively. The left hand side profiles show images taken at four different times during the experiment, and the right hand side profiles show computation results at the same times. Overall agreement between the two spreading patterns is good.

## CALIBRATION OF FLOW RESISTANCE COEFFICIENT

The flow resistance coefficient,  $C_D$ , is the only calibration parameter in this numerical model. This coefficient can be directly estimated from the measurements of velocity profiles. In this paper, the value of  $C_D$ , which will be used in the computation, is sought by a calibration. Experimental data in DEN5 (Table 2)

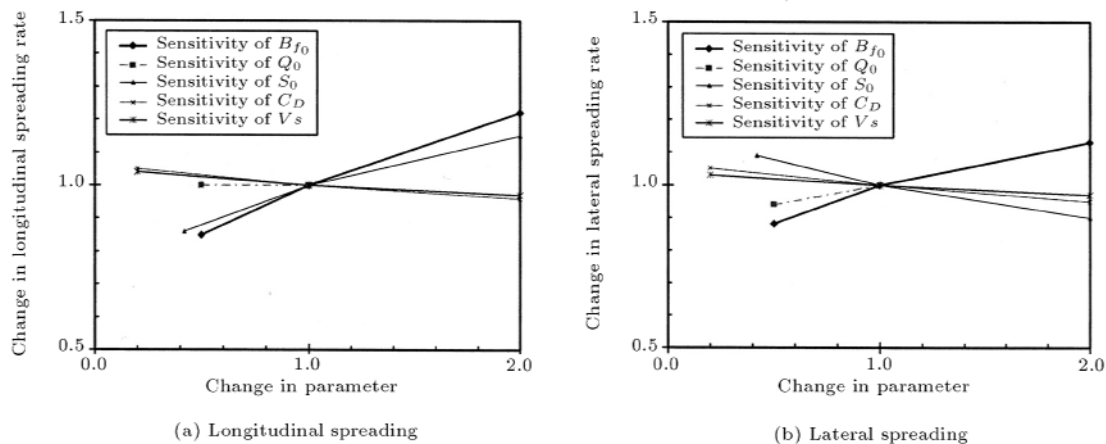
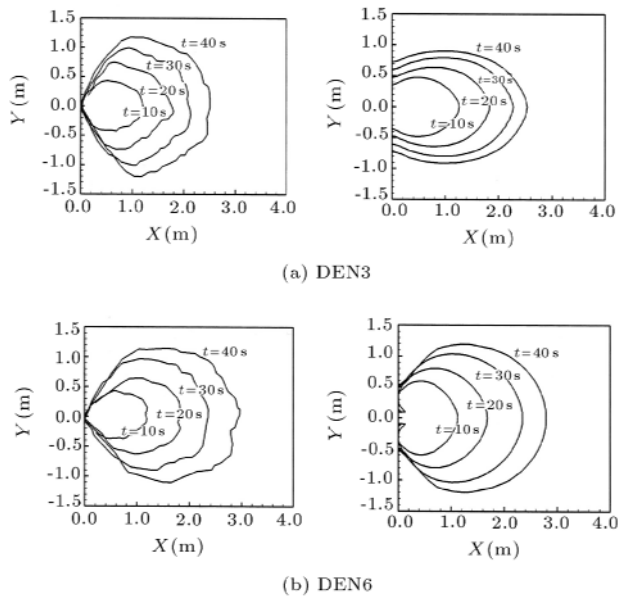


Figure 7. Sensitivity analysis of two-dimensional spreading upon parameters.



**Figure 8.** Comparison of spreading profiles in top view. (The left hand figures are the image taken from the experiment and the right hand side ones are the numerical computation results at  $t = 10$  s, 20 s, 30 s and 40 s.)

have been selected for calibration and the simulation results are shown in Figure 9. It is seen that the higher the value of  $C_D$ , the slower the propagation in both directions, as discussed in the sensitivity analysis. Comparing the computed results with the measured data from DEN5, a value of  $C_D = 0.005$  has been yielded as the best agreement for both longitudinal and lateral spreading. Therefore, a constant value of  $C_D = 0.005$  is selected for the computation of density currents. In addition, this value of  $C_D$  falls well within the range of values from the measurements by Parker et al. [28] and Garcia and Parker [20].

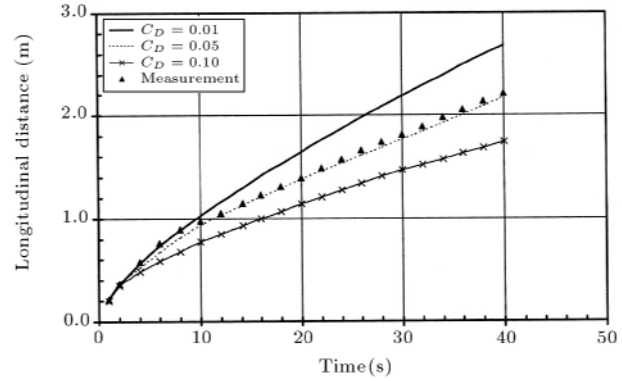
## CONCLUSION

Density currents in reservoirs depend on many parameters. Several numerical tests were performed in this paper to investigate those parameters, based on experimental and theoretical results. It was shown that they can change the mixture, the transport distance of solid material, the amount of sedimentation and the erosion of the bed.

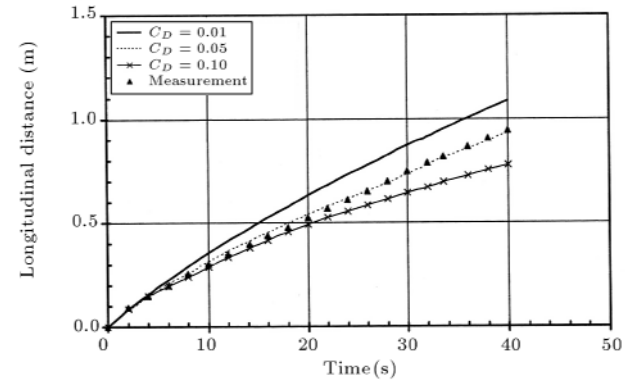
A finite volume two-dimensional numerical model

**Table 2.** Summary of experimental conditions.

Test Case	Discharge ( $\text{cm}^2/\text{s}$ )	$h_0$ (cm)	Bed Slope Angle	Concentration
DEN3	50	3	2	0.0121
DEN5	50	3	5	0.006
DEN6	50	3	5	0.0121



(a) Longitudinal spreading



(b) Lateral spreading

**Figure 9.** Calibration of flow resistance coefficient.

was developed for the analysis of unsteady turbidity (or density) currents. The Exner equation was used to model the bed-level changes, due to erosion and the deposition of suspended sediment. The developed numerical model was then used to simulate the experimental cases of 1D and 2D turbidity currents. In the one-dimensional case, the results obtained from the numerical model were compared with the experimental data of Altinakar et al. [41] and Garcia [43]. The numerical model for two-dimensional turbidity currents was applied to a laboratory experiment by Luthi [44]. The laboratory experiments of Choi [45] were employed for verification of the two-dimensional numerical model. The computed flow patterns were similar to experimental measurements. The two-dimensional spreading patterns and profiles of the velocity vectors and concentrations were obtained for a decelerating-depositional turbidity current. Favorable agreement was achieved between the simulated and measured values. These results demonstrated that the developed numerical model is capable of predicting the longitudinal and lateral spreading and dilution of turbidity currents. The proposed model is, thus, potentially useful to study the impact of turbidity currents on reservoir sedimentation and to simulate the sedimentary architecture of sea beds.

## ACKNOWLEDGMENT

This work has been funded by the Water Research Institute at the Ministry of Energy, I.R. Iran.

## REFERENCES

1. Turner, J.S., *Buoyancy Effects in Fluids*, Cambridge University Press, Cambridge, UK, p 367 (1973).
2. García, M. "Depositing and eroding sediment-driven flows: Turbidity currents", University of Minnesota, St. Anthony Falls Hydraulic Laboratory, Project Report No. 306, Minneapolis, Minnesota (1990).
3. Tsihrintzis, V.A. and Alavian, V. "Spreading of three-dimensional inclined gravity plumes", *J. Hyd. Res.*, **34**(5), pp 695-711 (1996).
4. Simpson, J.E. "Gravity currents in the laboratory, atmosphere, and ocean", *Ann. Rev. Fluid Mech.*, **14**, p 213 (1982).
5. Mulder, T. and Syvitsky, J. "Turbidity currents generated at river mouths during exceptional discharges to the world oceans", *J. Geology*, **103**, pp 285-299 (1995).
6. Parker, G., Fukushima, Y. and Pantin, H.M. "Self-accelerating turbidity currents", *J. Fluid Mech.*, **171**, pp 145-181 (1986).
7. García, M. "Turbidity currents", *Encyclopedia of Earth Sc.*, **4**, pp 399-407 (1992).
8. Hay, A.E. "Turbidity currents and submarine channel formulation in Rupert Inlet, British Columbia 1. Surge observations", *J. Geophys. Res.*, **92**, pp 2875-2881 (1987a).
9. Forel, F.A. "Théorie du ravin sous-lacustre", *Le Léman*, **1**, pp 381-386, publ. F. Rouge, Lausanne, Switzerland (1982).
10. Lambert, A. "Turbidity currents from the Rhine River on the bottom of Lake Constance", *Wasserwirtschaft*, **72**(4), pp 1-4 (in German) (1982).
11. Lambert, A. and Giovanoli, F. "Records of river borne turbidity currents and indications of slope failures in the Rhone delta of Lake Geneva", *Limnology and Oceanography*, **33**(3), pp 458-468 (1988).
12. Ellison, T.H. and Turner, J.S. "Turbulent entrainment in stratified flows", *J. Fluid Mech.*, Cambridge, England, **6**, pp 423-448 (1959).
13. Simpson, J.E. and Britter, R.E. "The dynamics of the head of a gravity current advancing over a horizontal surface", *J. Fluid Mech.*, **94**, pp 477-495 (1977).
14. Britter, R.E. and Linden, P.F. "The motion of the front of a gravity current traveling down an incline", *J. Fluid Mech.*, **99**, pp 531-543 (1980).
15. Middleton, G.V. "Experiments on density and turbidity currents, III. Deposition of sediment", *Canadian J. Earth Science*, **4**, pp 297-307 (1967).
16. Siegenthaler, C. and Buhler, J. "The kinematics of turbulent suspension currents (turbidity currents) on inclined boundaries", *Mar. Geol.*, **64**, pp 19-40 (1985).
17. García, M. "Depositing and eroding sediment-driven flows: Turbidity currents", University of Minnesota, St. Anthony Falls Hydraulic Laboratory Project Report No. 306., Minneapolis, Minnesota (1990).
18. García, M. "Depositional turbidity current laden with poorly sorted sediment", *J. Hyd. Eng.*, **120**(11), pp 1240-1263 (1994).
19. García, M. and Parker, G. "Experiment of bed sediment into suspension", *J. Hyd. Eng.*, **117**(4), pp 414-435 (1991).
20. García, M. and Parker, G. "Experiments on the entrainment of the sediment into suspension by a dense bottom current", *J. Geophys. Res.*, **98**(C3), pp 4793-4807 (1993).
21. Stefan, H. "High concentration turbidity currents in reservoirs", *Proc. 15th Conf., IAHR*, **1**, pp 341-352 (1973).
22. Ashida, K. and Egashira, S. "Basic study of turbidity currents", *Proc. Japan Soc. of Civil Eng.*, **237**, pp 37-50 (1975).
23. Feitz, T.R. and Wood, I.R. "Three dimensional density current", *J. Hyd. Div., ASCE*, **93**(HY6), pp 1-23 (1967).
24. Pantin, H.M. "Interaction between velocity and effective density in turbidity flow: Phase-plane analysis with criteria for autosuspension", *Mar. Geol.*, **31**, pp 59-99 (1979).
25. Lüthi, S. "Some new aspects of two-dimensional turbidity currents", *Sedimentology*, **28**, pp 97-105 (1980).
26. Parker, G. "Conditions for the ignition of catastrophically erosive turbidity currents", *Mar. Geol.*, **46**, pp 307-327 (1982).
27. Fukushima, Y., Parker, G. and Pantin, H.M. "Prediction of ignitive turbidity currents in Scripps submarine canyon", *Mar. Geol.*, **67**, pp 55-81 (1985).
28. Parker, G. et al. "Experiments on turbidity currents over an erodible bed", *J. Hydr. Res.*, Delft, The Netherlands, **25**(1), pp 123-147 (1987).
29. Hay, A.E. "Turbidity currents and submarine channel formation in Rupert Inlet, British Columbia, 2. The roles of continuous and surge type flow", *J. Geophys. Res.*, **92**(c3), pp 2883-2900 (1987b).
30. Stacey, M.W. and Bowen, A.J. "The vertical structure of density and turbidity currents: Theory and observations", *J. Geophysical Res.*, **93**(C4), pp 3528-3542 (1988a).
31. Stacey, M.W. and Bowen, A.J. "The vertical structure of density and turbidity currents and a necessary condition for self-maintenance", *J. Geophysical Res.*, **93**(C4), pp 3543-3553 (1988b).
32. Eidsvik, K.J. and Brørs, B. "Self-accelerated turbidity current prediction based upon  $k-\varepsilon$  turbulence", *Cont. Shelf Res.*, **9**(7), pp 617-627 (1989).
33. Takahata, S. "A numerical model of turbidity currents", M.S. Thesis, Dept. of Civil Eng., University of Minnesota, Minneapolis (1995).

34. Mulder, T., Savoye, P. and Syvitski, J. "Numerical modeling of a mid-sized gravity flow: the 1979 nice turbidity current (dynamics, process, sediment budget and seafloor impact)", *Sedimentology*, **44**(2), pp 305-326 (1997).
35. Salaheldin, T.M., Imran, J., Chaudhry, M.H. and Reed, C. "Role of fine sediments in turbidity current flow dynamics and resulting deposits", *Marine Geology*, **171**, pp 21-38 (2000).
36. Simpson, J.E., *Gravity Currents in the Environment and the Laboratory*, Cambridge University Press, 2nd edition (1997).
37. Simpson, J.E., *Gravity Currents*, Cambridge University Press, Cambridge, United Kingdom (1997).
38. Graf, W.H. and Altinakar, M.S. "Turbidity currents", *Fluvial Hydraulics-Flow and Transport, Processes in Channels of Simple Geometry*, Wiley, Chapter 7, New York, USA, pp 469-516 (1998).
39. Choi, S.U. and García, M.H. "Arbitrary Lagrangian-Eulerian approach for finite element modeling of two-dimensional turbidity currents", *Water International Journal*, **21**, pp 175-182 (1996).
40. Choi, S.U. and Garcia, M. "Modeling of one-dimensional turbidity current with a dissipative-Galerkin finite element method", *J. of Hyd. Research*, **33**(5), pp 623-648 (1995).
41. Altinakar, M.S., Graf, W.H. and Hopfinger, E.J. "Weakly depositing turbidity current on a small slope", *Journal of Hydraulic Research*, **28**, pp 55-80 (1990).
42. Bradford, S.F. and Katopodes, N.D. "Hydrodynamics of turbid underflows, II: Aggradation, avulsion and channelization", *J. Hyd. Eng., ASCE*, **125**(10), pp 1016-1028 (1999).
43. García, M. "Hydraulic jumps in sediment-driven bottom currents", *J. Hyd. Eng., ASCE*, **119**(10), pp 1094-1117 (1993).
44. Lüthi, S. "Experiments on non-channelized turbidity current and their deposits", *Marine Geology*, **40**, pp M59-M68 (1981).
45. Choi, S.U. "Layer averaged modeling of two-dimensional turbidity current with a dissipative-Galerkin finite element method", *J. Hyd. Research*, **33**(5), pp 623-648 (1998).